AMERICAN SOCIETY FOR MICROBIOLOGY | Journal of Virology®

VACCINES AND ANTIVIRAL AGENTS

CD4+ T Cells Drive Lung Disease Enhancement Induced by Immunization with Suboptimal Doses of Respiratory Syncytial Virus Fusion Protein in the Mouse Model

Kirsten Schneider-Ohrum,[a]* Angie Snell Bennett,[a] Gaurav Manohar Rajani,[a] Leigh Hostetler,[b] Sean K. Maynard,[a] Michelle Lazzaro,[a] Lily I. Cheng,[c] Terrence O'Day,[d] Corinne Cayatte[a]

[a]Department of Infectious Disease/Vaccines, MedImmune, Gaithersburg, Maryland, USA
[b]Laboratory Animal Resources, MedImmune, Gaithersburg, Maryland, USA
[c]Pathology Department, MedImmune, Gaithersburg, Maryland, USA
[d]Statistical Sciences, MedImmune, Gaithersburg, Maryland, USA

ABSTRACT Respiratory syncytial virus (RSV) infection of seronegative children previously immunized with formalin-inactivated (FI) RSV has been associated with serious enhanced respiratory disease (ERD). The phenomenon was reproduced in the cotton rat and the mouse, and both preclinical models have been routinely used to evaluate the safety of new RSV vaccine candidates. More recently, we demonstrated that immunizations with suboptimal doses of the RSV fusion (F) antigen, in its post- or prefusion conformation, and in the presence of a Th1-biasing adjuvant, unexpectedly led to ERD in the cotton rat model. To assess if those observations are specific to the cotton rat and to elucidate the mechanism by which vaccination with low antigen doses can drive ERD post-RSV challenge, we evaluated RSV post-F antigen dose de-escalation in BALB/c mice in the presence of a Th1-biasing adjuvant. While decreasing antigen doses, we observed an increase in lung inflammation associated with an upregulation of proinflammatory cytokines. The amplitude of the lung histopathology was comparable to that of FI-RSV-induced ERD, confirming the observations made in the cotton rat. Importantly, depletion of CD4+ T cells prior to viral challenge completely abrogated ERD, preventing proinflammatory cytokine upregulation and the infiltration of T cells, neutrophils, eosinophils, and macrophages into the lung. Overall, low-antigen-dose-induced ERD resembles FI-RSV-induced ERD, except that the former appears in the absence of detectable levels of viral replication and in the context of a Th1-biased immune response. Taken together, our observations reinforce the recent concept that vaccines developed for RSV-naïve individuals should be systematically tested under suboptimal dosing conditions.

IMPORTANCE RSV poses a significant health care burden and is the leading cause of serious lower-respiratory-tract infections in young children. A formalin-inactivated RSV vaccine developed in the 1960s not only showed a complete lack of efficacy against RSV infection but also induced severe lung disease enhancement in vaccinated children. Since then, establishing safety in preclinical models has been one of the major challenges to RSV vaccine development. We recently observed in the cotton rat model that suboptimal immunizations with RSV fusion protein could induce lung disease enhancement. In the present study, we extended suboptimal dosing evaluation to the mouse model. We confirmed the induction of lung disease enhancement by vaccinations with low antigen doses and dissected the associated immune mechanisms. Our results stress the need to evaluate suboptimal dosing for any new RSV vaccine candidate developed for seronegative infants.

KEYWORDS GLA-SE, RSV, RSV F, suboptimal vaccine, enhanced RSV disease

Citation Schneider-Ohrum K, Snell Bennett A, Rajani GM, Hostetler L, Maynard SK, Lazzaro M, Cheng LI, O'Day T, Cayatte C. 2019. CD4+ T cells drive lung disease enhancement induced by immunization with suboptimal doses of respiratory syncytial virus fusion protein in the mouse model. J Virol 93:e00695-19. https://doi.org/10.1128/JVI.00695-19.

Editor Terence S. Dermody, University of Pittsburgh School of Medicine

Address correspondence to Corinne Cayatte, cayattec@medimmune.com.

* Present address: Kirsten Schneider-Ohrum, GSK Vaccines, Rockville, Maryland, USA.

Received 25 April 2019
Accepted 8 May 2019
Accepted manuscript posted online 15 May 2019
Published 17 July 2019

Respiratory syncytial virus (RSV) causes lower-respiratory-tract infections leading to mortality and morbidity in children, the elderly, and immunocompromised adults and therefore represents a significant public health issue and economic burden (1–3). The only FDA-approved treatment for high-risk infants consists of a prophylactic administration of palivizumab, a monoclonal antibody (MAb) targeting the surface fusion (F) glycoprotein, which mediates viral entry and propagation in the host (4). However, the current cost of this MAb prophylaxis, along with the inconvenience of once-a-month injections, makes immunoprophylaxis with palivizumab unfeasible for healthy infants and warrants the development of a RSV vaccine.

The major obstacle to vaccine development dates from the 1960s with the failure of an alum-precipitated, formalin-inactivated (FI) RSV vaccine candidate that, in addition to lacking efficacy, induced enhanced respiratory disease (ERD) upon natural infection (5–8). This led to the deaths of two children and to the hospitalization of 80% of the vaccinees, as opposed to 5% in the control vaccine group. ERD included pneumonia, bronchiolitis, rhinitis, and bronchitis, despite an encouraging initial $\geq$4-fold increase in the level of neutralizing antibodies (NAbs) in 43% of the vaccinees (8). A more-detailed study on the composition of the anti-RSV antibodies showed poor neutralizing activity against the F and G viral surface glycoproteins relative to that in naturally infected individuals. The authors concluded that FI-RSV induced an unbalanced immune response, with an unusual proportion of non-neutralizing antibodies against the F and G antigens (9).

Additionally, postmortem examination of the lungs from the two fatal cases revealed the presence of mononuclear cells, neutrophils, and eosinophils in the lower respiratory tract. It was hypothesized that alum-precipitated FI-RSV vaccination primed for an exaggerated Th2-biased immune response in the absence of cytotoxic T lymphocytes (reviewed in references 10 and 11), which, upon subsequent RSV exposure, led to high antigen burdens in the lungs and to the recruitment of immune cells (i.e., RSV-specific T cells, neutrophils, or eosinophils), ultimately resulting in airway obstruction.

The RSV F glycoprotein, in its postfusion (RSV post-F) or prefusion (RSV pre-F) conformation (12), is the primary target for neutralizing antibodies and the antigen of choice for vaccine development due to its antigenic stability, with minimal differences between RSV subtypes (13). Numerous studies in animal models have suggested that a safe immune profile in response to RSV immunization should combine a highly neutralizing antibody response with a Th1-biased cellular response (reviewed in references 14 and 15). However, we have reported that in the cotton rat model, vaccination with suboptimal doses of soluble RSV F (sF) antigen (in the post- or prefusion conformation) in the presence of a strong Th1-biasing adjuvant (GLA-SE, comprising a Toll-like receptor 4 [TLR4] agonist, glucopyranosyl lipid A [GLA], integrated into a stable squalene emulsion [SE]) could also lead to alveolitis-associated histopathology, the hallmark of ERD (16). Due to the lack of availability of immunological tools for the cotton rat, the exact mechanism of action of low-antigen-dose-associated ERD could not be investigated.

In the present study, we conducted a detailed immunological evaluation of soluble RSV post-F antigen dose de-escalation in order to evaluate whether low antigen doses could also lead to ERD in the BALB/c mouse model. The inflammation profiles induced by low antigen doses post-RSV A2 challenge were compared to those in FI-RSV-induced enhanced disease. In order to elucidate the potential mechanism of action leading to ERD, we depleted $CD4^+$ and $CD8^+$ T cells prior to viral challenge and evaluated the impact on subsequent lung inflammation.

Interestingly, we confirmed our initial observations made in the cotton rat model (16): low doses of RSV post-F antigen, even in the presence of a Th1-biasing adjuvant, induce lung histopathology similar to that with FI-RSV. Despite different immunological profiles induced by FI-RSV (Th2 bias) and low RSV F antigen doses (Th1 bias), $CD4^+$ T cell depletion completely prevented ERD in both instances, strongly inhibiting lung inflammation and immune cell infiltration, whereas $CD8^+$ T cell depletion had only a

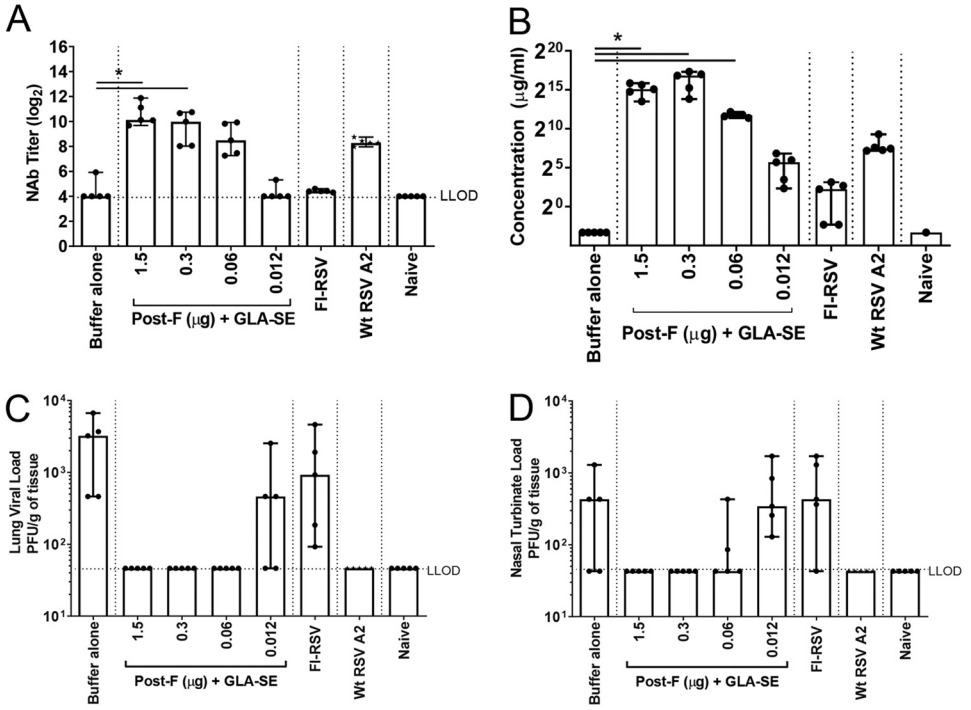

FIG 1 Immunogenicity induced by decreasing doses of post-F antigen. BALB/c mice (7 weeks old; *n*, 5 per group) were immunized i.m. at day 0 and day 21 with either buffer alone, different doses of post-F antigen with GLA-SE (2.5 μg GLA in 2% SE) as an adjuvant, or FI-RSV. A control group for natural infection was immunized i.n. with live RSV (10^6 PFU) at day 0. At day 34, animals were challenged i.n. with 10^6 PFU of wild-type (wt) RSV A2. Naïve animals were left untreated. (A) Prior to challenge (day 33), sera were harvested, and NAb titers were evaluated using a microneutralization assay. Data are presented as the $\log_2$ dilution of serum that provides a 50% reduction in viral entry with an LLOD of 4 (indicated by a dashed line). (B) At sacrifice (day 39), RSV F-specific total IgG was measured by ELISA. For panels A and B, Kruskal-Wallis analyses comparing the experimental groups with the buffer-alone group were performed, followed by pairwise Dunn's multiple-comparison tests. *, $P < 0.05$. (C and D) Lung (C) and nasal turbinate (D) viral loads were determined by plaque assays. Medians, with ranges of individual values, are shown.

marginal impact. Overall, the confirmation of low-antigen-dose-induced ERD in a model other than the cotton rat and the elucidation of its mechanism of action are of great importance for the RSV field. The present work will help to guide the preclinical evaluation of any new vaccine candidate targeting RSV-naïve infants and children.

RESULTS

RSV F-specific antibody response and lung protection from viral challenge after immunization with decreasing doses of soluble RSV post-F antigen. BALB/c mice were immunized twice (day 0 and day 21) intramuscularly (i.m.) with an antigen dose that conferred full protection in previous studies (1.5 μg) or with decreasing doses of RSV post-F antigen (0.3, 0.06, and 0.012 μg) in the presence of the GLA-SE adjuvant (2.5 μg GLA in 2% SE) (Fig. 1). As expected, immunization with decreasing doses of antigen resulted in decreasing levels of neutralizing antibody (NAb) titers (means, 10.6, 9.5, 8.6, and 4.3 $\log_2$, respectively) (Fig. 1A) and decreasing concentrations of anti-RSV F-specific total IgG (ranging from 2^{15} to 2^5 μg/ml) (Fig. 1B). Only the lowest antigen dose tested (0.012 μg) failed to induce an immune response that conferred full protection against RSV A2 challenge in the lungs; viral breakthrough was observed in 3 animals out of 5 (Fig. 1C). Similarly, FI-RSV immunization induced low NAb titers (mean, 4.4 $\log_2$) and low concentrations of anti-RSV F-specific IgG (2^2 μg/ml) and failed to raise an immune response capable of conferring complete protection from viral replication in the lungs; viral titers were measurable in all animals (Fig. 1). Additionally, measurement of viral titers in nasal turbinates (NT) (Fig. 1D) showed that the two doses below 0.3 μg of antigen did not confer full protection in the upper respiratory tract and

are therefore considered suboptimal in the context of immunization with RSV F plus GLA-SE in mice.

Overall, profiles similar to those published previously for the cotton rat model (16) were obtained, with antigen doses covering full to no protection of the lungs from challenge.

Dosing down of soluble RSV post-F antigen leads to enhanced inflammation in lung tissue post-RSV A2 challenge. Lungs from animals immunized with decreasing doses of RSV post-F antigen or with FI-RSV, a positive control for ERD, were harvested 4 days post-RSV A2 challenge, homogenized, and clarified by centrifugation, and the supernatants were pooled for each treatment group and were analyzed in duplicate by multiplex cytokine analysis. The expression of cytokines previously associated with FI-RSV-induced enhanced disease (eotaxin, interleukin 5 [IL-5], IL-13, and tumor necrosis factor alpha [TNF-α]) (17–19) was assessed (Fig. 2A to D). As expected, the Th2-biasing cytokines IL-5, IL-13, and eotaxin were strongly upregulated in animals previously immunized with FI-RSV relative to levels in animals immunized with the optimal dose of RSV F (1.5 μg), with 95-, 114-, and 8-fold increases, respectively. TNF-α was also induced in FI-RSV-immunized animals, but to a lesser extent under these experimental conditions (a 3.3-fold increase over the level with 1.5 μg of RSV F plus GLA-SE). Interestingly, IL-5 and eotaxin were only mildly upregulated by immunization with low doses of RSV F antigen, peaking at the RSV post-F dose of 0.06 μg with 8- and 2-fold increases, respectively, over levels with RSV F at the 1.5-μg dose. IL-13 was undetectable in all RSV F-immunized animals, and TNF-α upregulation was similar to that observed in the FI-RSV group (a 2.2-fold increase). Overall, the data suggest potential differences between the pathway leading to ERD induced by FI-RSV and that for ERD induced by low RSV F antigen doses.

The cytokine analysis was extended to other proinflammatory cytokines (IL-6, interferon gamma-induced protein 10 [IP-10], and monocyte chemoattractant protein 1 [MCP-1]) and to cytokines with neutrophil chemoattractant properties (IL-17, keratinocyte chemoattractant [KC], and macrophage inflammatory protein 2 [MIP-2]) (Fig. 2E to J) (20). All of these cytokines were upregulated at lower doses of RSV F antigen (peaking at 0.06 μg in this experiment, with 6.3-, 9.1-, 3.6-, 4.1-, 2.5-, and 2-fold increases, respectively). In contrast, FI-RSV induced only IL-6 and MIP-2 (8- and 2.1-fold, respectively), suggesting, again, potentially different mechanisms for inflammation enhancement triggered by FI-RSV and that triggered by immunization with a low dose of RSV F.

Vaccination with low RSV post-F antigen doses induces enhanced lung pathology. To evaluate the impact of the observed increase in inflammatory cytokines induced by low RSV F doses on lung histopathology, we focused our investigation on three doses of RSV F antigen (1.5, 0.06, and 0.012 μg) (Fig. 3). To further confirm that our observations were specifically correlated with RSV F antigen vaccination, another negative control was introduced, consisting of a group of animals immunized with a nonrelevant antigen, human cytomegalovirus (CMV) glycoprotein B (gB; 0.06 μg) with GLA-SE (2.5 μg GLA in 2% SE) as an adjuvant. Four days post-RSV A2 challenge, lungs were harvested, inflated with 10% formalin, and embedded in paraffin. Sections stained with hematoxylin and eosin (H&E) were examined and scored by a blinded pathologist. A cumulative histopathology score ranging from 0 to 20 was based on inflammatory characteristics including (i) peribronchiolar cuffing by lymphocytes and/or neutrophils, (ii) alveolitis (characterized by lymphocytes, macrophages, and neutrophils within alveolar spaces), and (iii) thickening of alveolar walls. Low histopathology scores (median score, 1.5) were observed in the buffer-alone negative-control group and, more importantly, in the negative-control group immunized with CMV gB plus GLA-SE, demonstrating that the GLA-SE adjuvant alone does not induce disease enhancement and that ERD is dependent on the RSV F antigen. Vaccination with 1.5 μg RSV F antigen with GLA-SE induced mild inflammation (median score, 5) (Fig. 3H). In contrast, significantly higher histopathology scores were observed in animals immunized with FI-RSV or with a low dose of RSV F antigen (0.06 μg); the median overall histopathology score

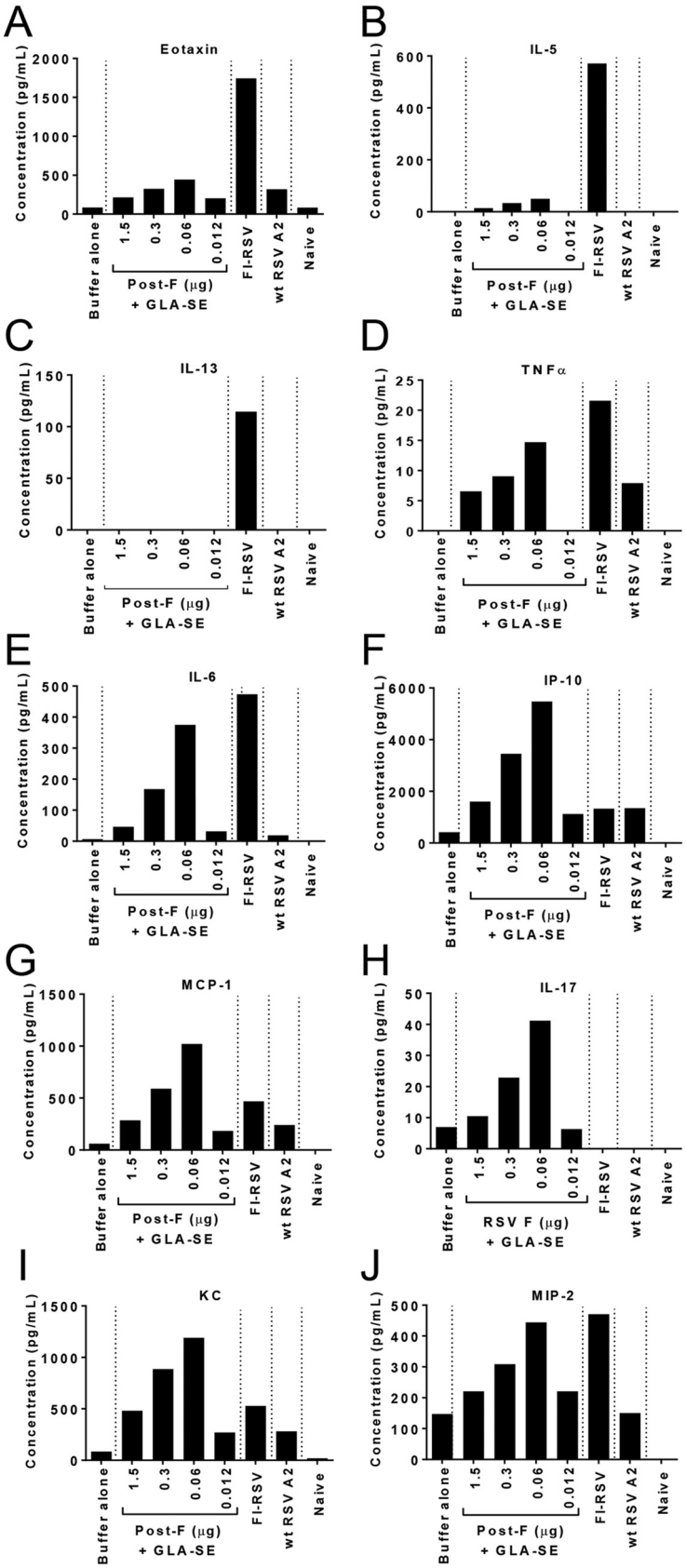

FIG 2 Dosing down of antigen leads to enhanced inflammation in lung tissue post-RSV A2 challenge. BALB/c mice (7 weeks old; *n*, 5 per group) were immunized i.m. at day 0 and day 21 with either buffer

(Continued on next page)

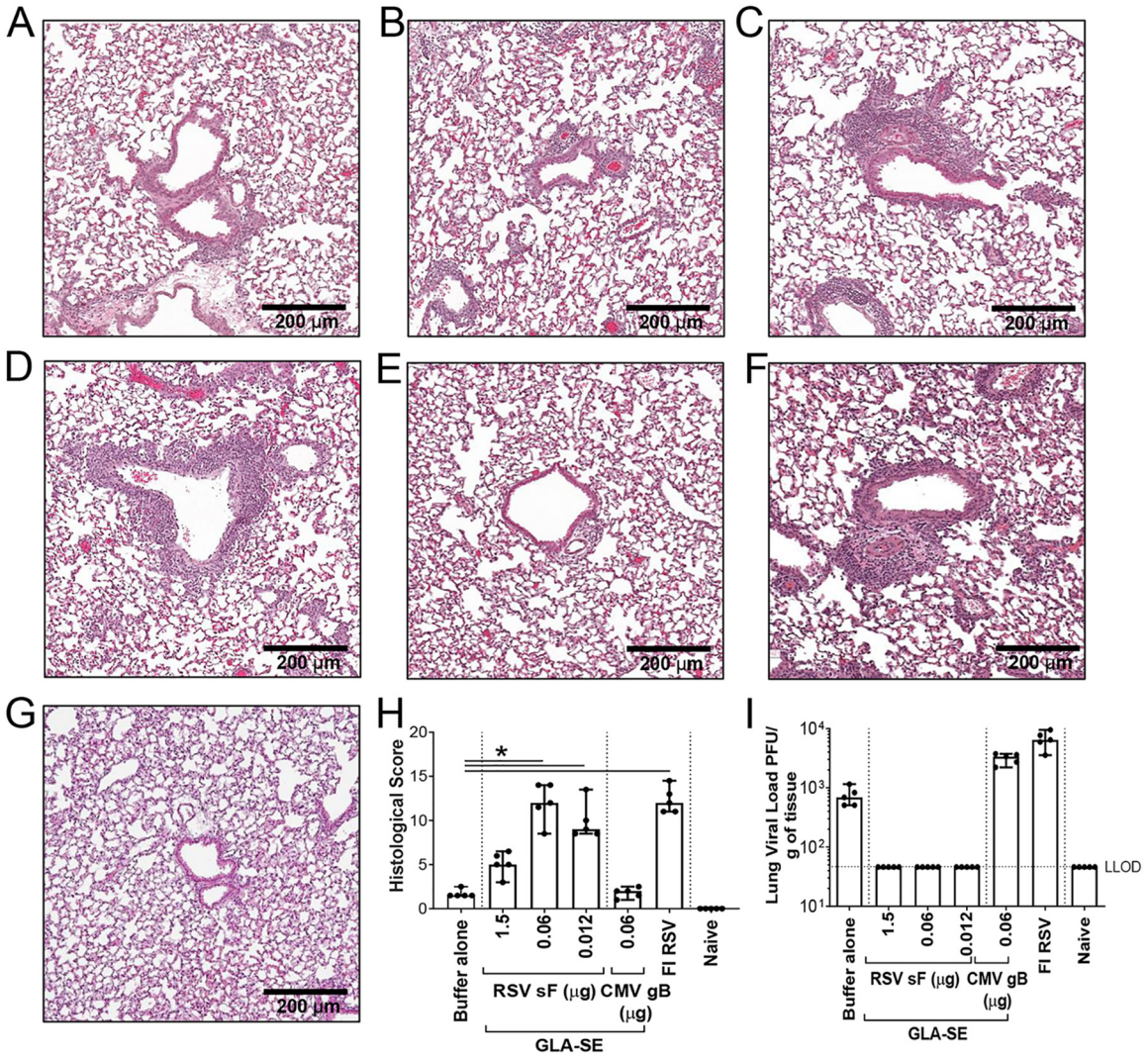

FIG 3 Vaccination with low antigen doses induces enhanced lung pathology. BALB/c mice (7 weeks old; *n*, 5 per group) were immunized i.m. at day 0 and day 21 with either buffer alone, different doses of post-F antigen with GLA-SE (2.5 μg GLA in 2% SE) as an adjuvant, or FI-RSV. A negative-control group was immunized with a nonrelevant antigen (CMV gB) with GLA-SE as an adjuvant. Naïve animals were left untreated. At day 34, animals were challenged i.n. with 10^6 PFU of wild-type (wt) RSV A2, and 4 days later, animals were sacrificed. Lungs were harvested, inflated with 10% formalin, and embedded in paraffin. Photomicrographs of H&E-stained sections are shown at $\times$10 magnification for animals vaccinated with either buffer alone (A), 1.5 μg RSV sF (B), 0.06 μg RSV sF (C), 0.0012 μg RSV sF (D), 0.06 μg CMV gB (E), or FI-RSV (F), and for naïve animals (G). (H) Lung histopathology was analyzed blindly by a trained pathologist; the combined scores (medians with ranges) for all groups are presented. Kruskal-Wallis analyses comparing the experimental groups with the buffer-alone group were performed on histological scores, except for the naïve score. Pairwise comparisons were performed with Dunn's multiple-comparison test. *, $P < 0.05$. (I) Lungs were homogenized, and viral titers were determined by plaque assays. Medians, with ranges of individual results, are shown. The horizontal dashed line indicates the lower limit of detection (LLOD).

was 12 for both treatment groups. In this experiment, the lowest dose of antigen (0.012 μg RSV F) also led to a high histopathology score, with no virus recovered in the lungs from those animals (Fig. 3I). Pronounced peribronchiolar and perivascular cuffing were noted, with an increase in the infiltration of lymphocytes and neutrophils, and the

FIG 2 Legend (Continued)
alone, different doses of post-F antigen with GLA-SE (2.5 μg GLA in 2% SE) as an adjuvant, or FI-RSV. A control group for natural infection was immunized i.n. with live RSV (10^6 PFU) at day 0. Naïve animals were left untreated. At day 34, animals were challenged i.n. with 10^6 PFU of wild-type (wt) RSV A2, and 4 days later, animals were sacrificed. Lungs were harvested, homogenized, clarified, pooled in each group, and analyzed by multiplex assays to assess the respective concentrations of eotaxin (A), IL-5 (B), IL-13 (C), TNF-α (D), IL-6 (E), IP-10 (F), MCP-1 (G), IL-17 (H), KC (I), and MIP-2 (J). The means of replicate measurements are shown.

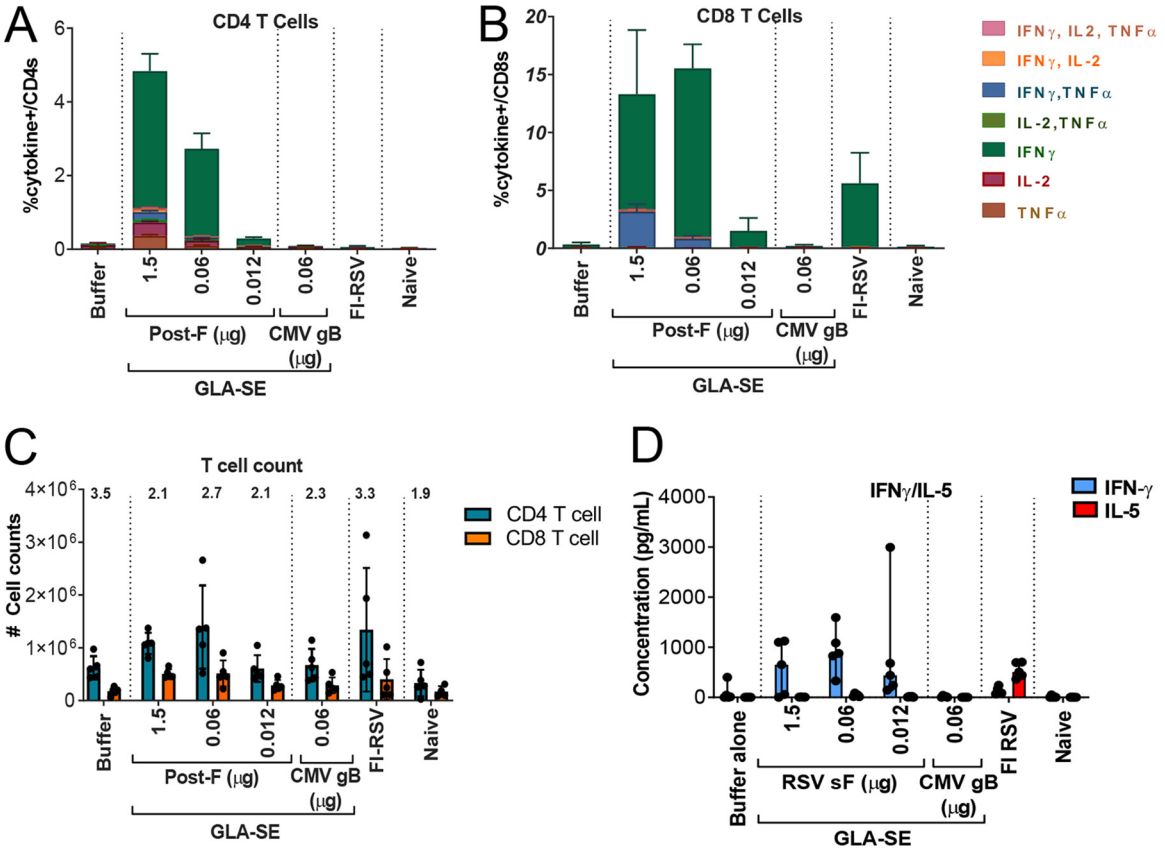

FIG 4 Dosing down of antigen does not alter lung RSV F-specific CD4+ and CD8+ T cell polyfunctionality, ratios, or Th1 bias. BALB/c mice (7 weeks old; *n*, 5 per group) were immunized i.m. at day 0 and day 21 with either buffer alone, different doses of post-F antigen with GLA-SE (2.5 μg GLA in 2% SE) as an adjuvant, or FI-RSV. A negative-control group was immunized with a nonrelevant antigen (CMV gB) with GLA-SE as an adjuvant. Naïve animals were left untreated. At day 34, animals were challenged i.n. with 10^6 PFU of wild-type (wt) RSV A2, and 4 days later, animals were sacrificed. Lung cells were isolated and were stimulated with an RSV F peptide pool to evaluate intracellular cytokine expression by flow cytometry. (A and B) Cells were surface stained with CD3 and CD8, intracellularly stained for IFN-γ, IL-2, and TNF-α, and analyzed on an LSR II instrument for the frequency of responding CD4+ (A) and CD8+ (B) T cells. The means of individual results ± standard errors of the means are shown. (C) Total CD4+ and CD8+ T cell counts were assessed, and the CD4/CD8 ratio is given above each bar. (D) Lungs from another set of animals were harvested and homogenized, and IFN-γ and IL-5 concentrations in the supernatant were evaluated by Luminex technology. Individual results and medians with ranges are shown in panels C and D.

presence of edema around the airways. This confirmed that inflammation induced by a low RSV F antigen dose was leading to histopathology characteristics similar to those of FI-RSV-induced ERD.

Dosing down of antigen does not alter RSV F-specific CD4+ and CD8+ polyfunctionality, CD4+/CD8+ T cell ratios, or Th1 bias in the lung. To investigate whether the inflammation and lung histopathology induced by lower antigen doses could be due to alteration of an RSV F-specific T cell activation profile or a change in Th1 bias, a detailed analysis was performed on lung cells from RSV F-vaccinated and FI-RSV-vaccinated animals after intranasal (i.n.) challenge with RSV A2 (Fig. 4).

Lung cells were isolated from the animals 4 days post-RSV A2 challenge and were stimulated overnight with overlapping RSV F peptide pools. The intracellular expression levels of gamma interferon (IFN-γ), IL-2, and TNF-α in CD4+ and CD8+ T cells were assessed using flow cytometry (Fig. 4A and B). RSV F-specific CD4+ T cells were mainly IFN-γ producers, and RSV F-specific CD8+ T cells were IFN-γ producers or IFN-γ–TNF-α double producers. As expected, lowering the antigen dose to 0.06 μg decreased the magnitudes of the specific CD4+ and CD8+ T cell responses (mean 16- and 9-fold decreases, respectively) but did not alter the intracellular cytokine profiles. No RSV F-specific CD4+ T cell response could be detected in the FI-RSV-vaccinated group.

Total CD4+/CD8+ T cell ratios were also evaluated and failed to show any significant differences between groups that could explain the enhanced inflammation observed

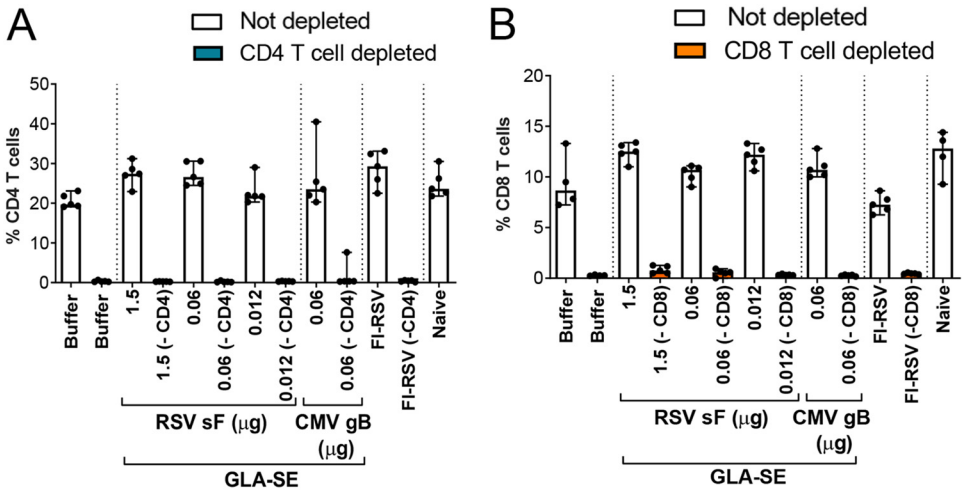

FIG 5 Impact of CD4$^+$ and CD8$^+$ T cell depletion in the lungs as assessed by flow cytometry. BALB/c mice (7 weeks old; *n*, 5 per group) were immunized i.m. at day 0 and day 21 with either buffer alone, different doses of post-F antigen with GLA-SE (2.5 μg GLA in 2% SE) as an adjuvant, or FI-RSV. A negative-control group was immunized with a nonrelevant antigen (CMV gB) with GLA-SE as an adjuvant. Naïve animals were left untreated. At days 29, 32, and 35, groups were treated i.p. with 250 μg of anti-CD4 (A) or anti-CD8 (B) antibodies as indicated. Four days after i.n. challenge with 10^6 PFU of wild-type (wt) RSV A2, animals were sacrificed. Lungs were harvested, and cells were isolated and surface stained as described in Materials and Methods. Individual results and medians with ranges are presented.

after vaccination with low antigen doses (Fig. 4C). Similarly, the Th1/Th2 profile in the lungs postchallenge was assessed (Fig. 4D) by measuring the relative amounts of IFN-γ and IL-5, and a clear Th1 profile was maintained at all antigen doses, as opposed to a Th2 profile in animals vaccinated with FI-RSV.

CD4$^+$ T cell depletion completely alters the cytokine profile induced by FI-RSV and low-dose RSV F immunizations post-RSV A2 challenge. For determination of the relative contributions of CD4$^+$ and CD8$^+$ T cells, specific depleting MAbs for each cell type were administered at day 29 (5 days prior to challenge), day 32 (2 days prior to challenge), and day 35 (1 day postchallenge) to ensure complete T cell depletion until sacrifice and lung harvest. The absence of CD4$^+$ and CD8$^+$ T cells in lung tissue was confirmed at the time of sacrifice, 4 days post-RSV A2 challenge, by flow cytometry (Fig. 5A and B, respectively).

Individual lung supernatants were also analyzed by multiplex cytokine analysis. We confirmed that the lung cytokine levels obtained from pooled samples (Fig. 2) were comparable to the means of measurements of unpooled samples (Fig. 6). Interestingly, CD4$^+$ T cell depletion had a pronounced effect on eotaxin, IL-5, IL-13, IL-17, and MIP-2 expression levels at all RSV F doses tested. The expression of these cytokines was similar to the low levels observed after vaccination either with buffer alone or with the CMV gB antigen control (Fig. 6A to C, H, and J). A similar observation was made in the case of vaccination with FI-RSV. With regard to the other cytokines evaluated, except for TNF-α, the main impact of CD4$^+$ T cell depletion was observed at the 0.012-μg dose of RSV F, which is the dose at which the cytokine expression levels were highest in that particular experiment (Fig. 6F, G, and I).

In contrast, the impact of CD8$^+$ T cell depletion was minor, and in some instances, even higher levels of inflammatory cytokines (for example, IL-13 and IL-17) were induced in the lung (Fig. 7).

CD4$^+$ T cell depletion strongly reduces the infiltration of inflammatory cells into the lungs postchallenge. To evaluate the correlation between lung cytokine levels and cell infiltration into the lungs postchallenge, lung cells were surface stained as described previously (21, 22) and were analyzed by flow cytometry (Fig. 8). CD4$^+$ T cell depletion reduced the infiltration of eosinophils, neutrophils, macrophages, and T cells, especially at the lowest RSV F antigen dose (0.012 μg) and in the FI-RSV-

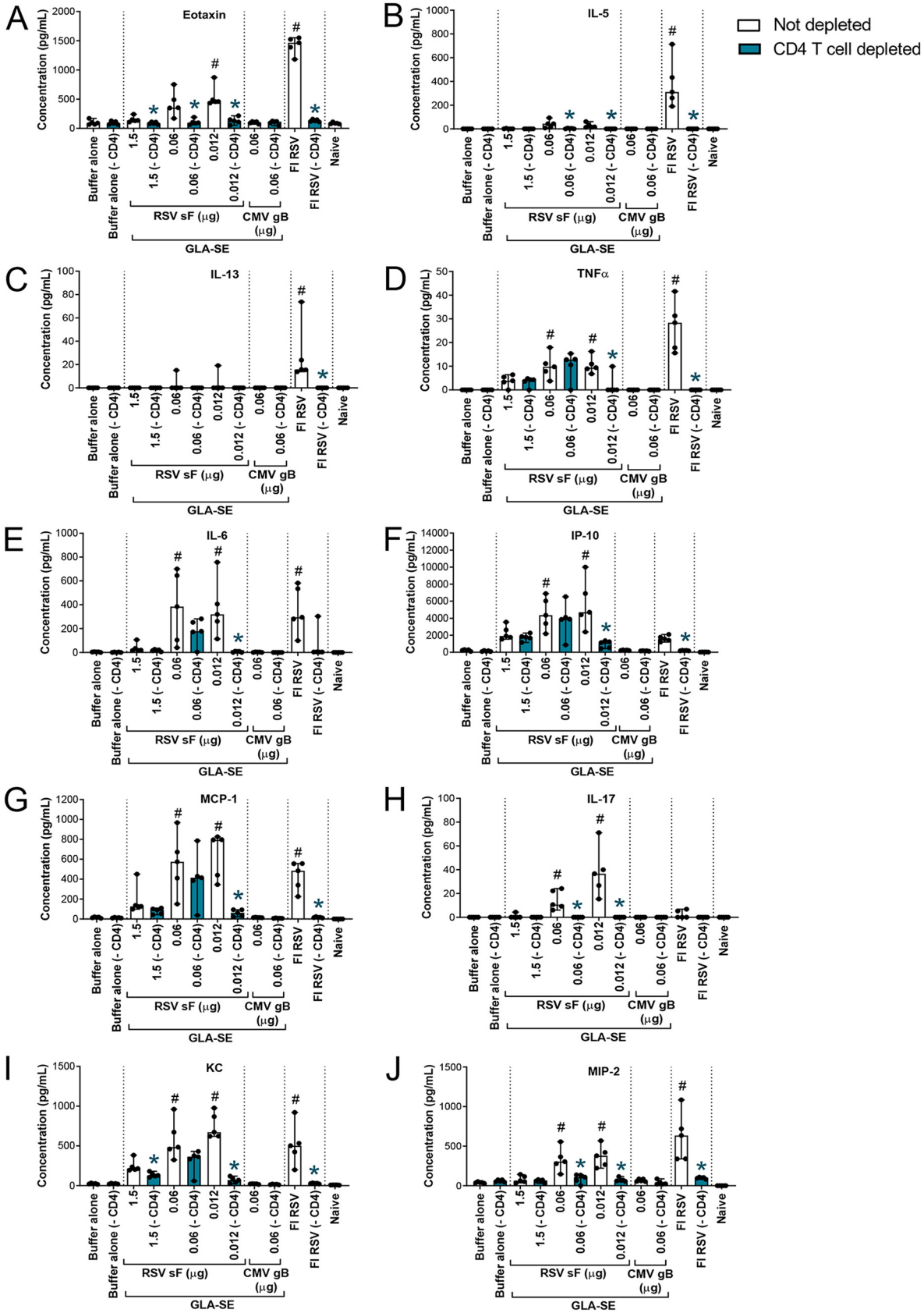

FIG 6 CD4+ T cell depletion has a strong impact on cytokines induced by FI-RSV or low-antigen-dose immunization post-RSV A2 challenge. BALB/c mice (7 weeks old; *n*, 5 per group) were immunized i.m. at day 0 and day 21 with either buffer alone, different doses of post-F antigen

(Continued on next page)

vaccinated group, to levels that were similar to those observed in animals vaccinated either with buffer alone or with the irrelevant CMV gB antigen.

Histological examination confirms that CD4$^+$ T cell depletion prevents enhanced lung pathology induced by vaccination with low RSV F antigen doses or FI-RSV. Finally, we examined whether the decrease in inflammatory cytokines and immune cell infiltration observed post-CD4$^+$ T cell depletion resulted in a decrease in the overall lung histopathology score (Fig. 9). The most significant impact was observed in FI-RSV-immunized animals and at the lowest dose of RSV F antigen (0.012 μg): median histopathology scores decreased from 12 to 3 and from 10 to 3, respectively (Fig. 9E). A score of 3, corresponding to minimal inflammation, was observed following immunization either with buffer alone or with the nonrelevant CMV gB antigen.

In sharp contrast, depletion of CD8$^+$ T cells did not significantly decrease the histopathology observed following immunization with FI-RSV and even increased the pathology score measured at the highest and lowest doses of RSV F antigen tested (Fig. 10).

DISCUSSION

Despite decades of efforts to establish a safe and efficient RSV vaccine, no subunit-based vaccine has entered clinical evaluation for seronegative infants, because of the fear of inducing disease enhancement, as was observed with the FI-RSV vaccine candidate in a clinical trial in the 1960s (8). Based on preclinical models recapitulating FI-RSV vaccine-induced ERD, it was believed that a strong Th1-biasing adjuvant and a purified recombinant antigen would be sufficient to provide safe immunity (reviewed in references 14 and 15). We showed in the cotton rat, the preferred model of reference for vaccine-induced ERD (23), that prophylactic doses of RSV F plus GLA-SE were protective, with no associated ERD signs post-RSV challenge, and that, in contrast, animals immunized with prophylactic doses of RSV F and an alum adjuvant exhibited clear signs of ERD (16). However, when we evaluated suboptimal immunizations by decreasing antigen doses to induce antibody titers below protective levels, surprisingly, we observed pronounced ERD in both the RSV F–GLA-SE and the RSV F–alum group post-RSV challenge (16), regardless of the addition of a Th1-biasing adjuvant. In the present study, we recapitulated and expanded our evaluation of RSV F with the GLA-SE adjuvant in the mouse model. We observed, as expected, that dosing down of antigen leads to a decrease in antigen-specific immunity for both humoral (Fig. 1) and cell-mediated (Fig. 4A and B) responses. Confirming the observations in the cotton rat model, we detected an increase in overall lung inflammation 4 days post-RSV challenge (Fig. 2; Fig. 4C and D) in the absence of detectable viral replication in the lungs of the animals (Fig. 3I) (16). Interestingly, the peak of inflammation fluctuated from experiment to experiment between 0.06-μg and 0.012-μg doses of RSV F but was consistently observed in the absence of detectable viral replication. Similar observations were made previously in the cotton rat model, with alveolitis occurring in the complete or almost complete absence of detectable virus in the lungs (16). In sharp contrast, FI-RSV-induced ERD was consistently observed in the presence of measurable replicating virus in the lungs in both the mouse and the cotton rat model. Even if no viral replication could be detected by plaque assays at the peak of inflammation, it is likely that low levels of virus were replicating, as indicated by detectable levels of virus in the upper respiratory tracts of animals immunized with low antigen doses (RSV F at 0.06 μg and

FIG 6 Legend (Continued)
with GLA-SE (2.5 μg GLA in 2% SE) as an adjuvant, or FI-RSV. A negative-control group was immunized with a nonrelevant antigen (CMV gB) with GLA-SE as an adjuvant. Naïve animals were left untreated. At days 29, 32, and 35, animals were treated i.p. with 250 μg of anti-CD4 antibodies. Four days after i.n. challenge with 10^6 PFU of wild-type (wt) RSV A2, animals were sacrificed. Lungs were homogenized and clarified, and individual supernatants were analyzed by multiplex assays to assess the respective concentrations of eotaxin (A), IL-5 (B), IL-13 (C), TNF-α (D), IL-6 (E), IP-10 (F), MCP-1 (G), IL-17 (H), KC (I), and MIP-2 (J). Individual results and medians with ranges are presented. Kruskal-Wallis analysis followed by Dunn's multiple-comparison tests were used for statistical analyses. Symbols indicate an adjusted *P* value of <0.05 for nondepleted conditions compared to buffer alone (#) or a *P* value of <0.05 for pairwise Mann-Whitney tests of nondepleted versus CD4 T cell-depleted conditions (*).

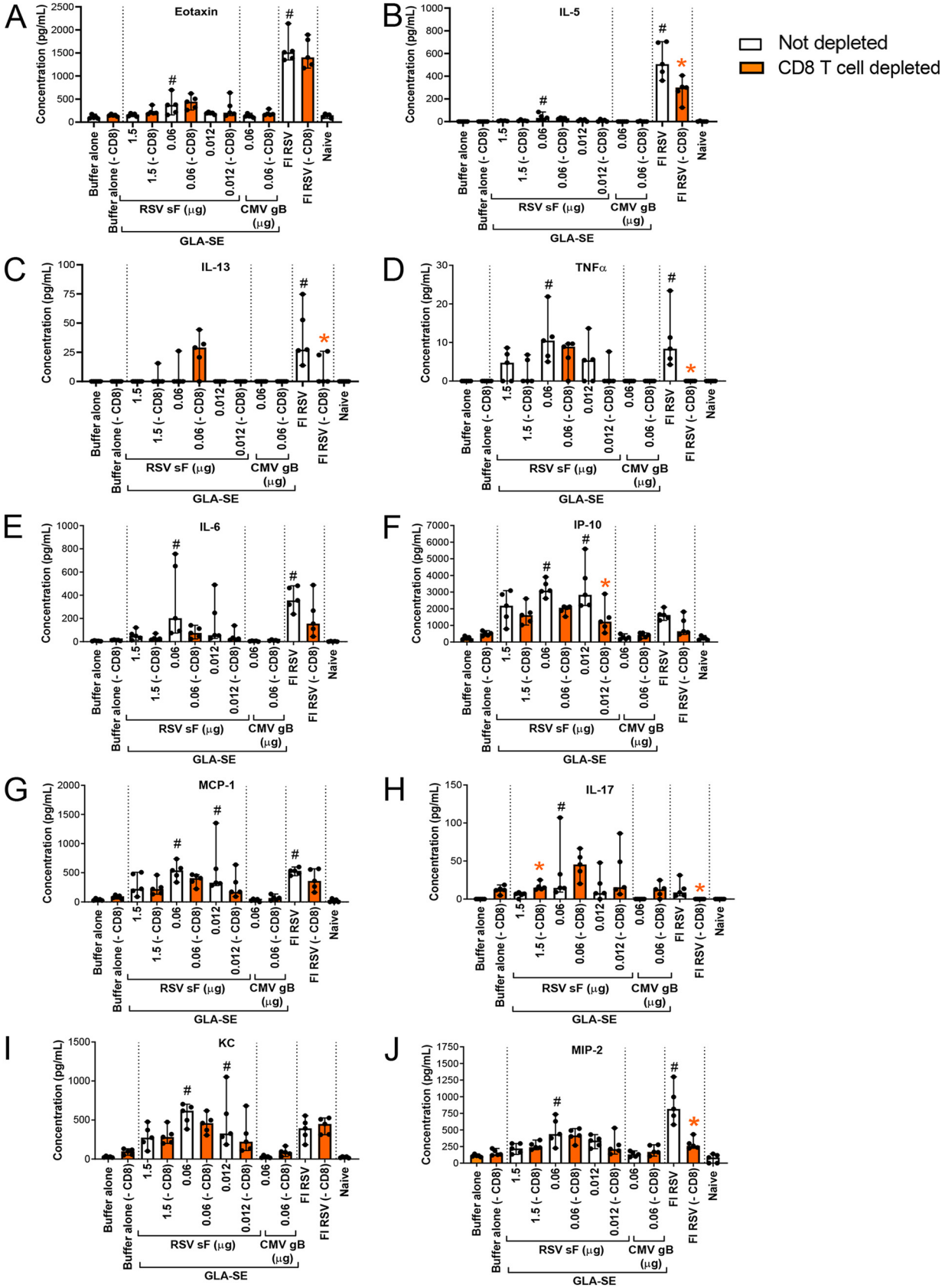

FIG 7 CD8+ T cell depletion has a mild impact on cytokines induced by FI-RSV or low-antigen-dose immunization followed by RSV A2 challenge. BALB/c mice (7 weeks old; *n*, 5 per group) were immunized i.m. at day 0 and day 21 with either buffer alone, different doses of post-F antigen with

(Continued on next page)

0.012 μg) (Fig. 1D). Additionally, it has been demonstrated that FI-RSV-induced ERD is dependent on viral replication (24).

A detailed analysis of lung-infiltrating cells showed increased levels of eosinophils, neutrophils, macrophages, and T cells with decreasing antigen doses, observations similar to those made for FI-RSV-immunized mice (Fig. 8). Eosinophilia is a characteristic of a Th2-mediated immune response and has been reported in the peripheral blood of many of the hospitalized children immunized with FI-RSV in the 1960s trial; more importantly, it was observed in the lungs of the two infants who tragically died (8). Lung eosinophilia is a prominent characteristic of FI-RSV-vaccinated mice challenged with RSV (9, 25–27), but it has been shown with eosinophil-deficient mice that eosinophils are actually not required to mediate FI-RSV pathology (19). Eosinophilia induced by immunization with low antigen doses was less pronounced than that in the FI-RSV-immunized group, a finding consistent with the lower levels of Th2-associated cytokines and chemokines (IL-5, IL-13, and eotaxin) observed with immunization with 0.06 μg RSV F and GLA-SE than with FI-RSV immunization. Lower antigen doses induced a more-pronounced neutrophil chemoattractant environment than FI-RSV, as indicated by higher levels of IL-17 and, to a lesser extent, KC (Fig. 2H and I; Fig. 6H and I; Fig. 7H and I). This also translated into higher neutrophil infiltrates in the lungs than in those of FI-RSV-immunized animals (Fig. 8). Interestingly, Zhang et al. recently reported that FI-RSV promoted Th17 responses and that Th17 inhibition through the stimulation of both TLR9 and Notch signaling pathways suppressed FI-RSV-induced ERD (28). In our model, $CD4^+$ T cell depletion dramatically reduced FI-RSV-induced ERD, as observed previously (27), but also inhibited ERD induced by low RSV F antigen doses, suggesting a potential common mechanism of vaccine-enhanced lung inflammation. $CD4^+$ T cell depletion had the most pronounced effect on Th2-associated cytokines/chemokines (eotaxin, IL-5, IL-13) (Fig. 6A to C) and on neutrophil chemoattractant cytokines (IL-17 and MIP-2) (Fig. 6H and J), which reverted to levels found in buffer-immunized control animals at all antigen doses tested. This implies that the expression of those cytokines/chemokines relies solely on the presence of $CD4^+$ T cells. Additionally, we observed that $CD4^+$ T cell depletion inhibited IL-6, IP-10, MCP-1, and KC expression only at the peak of inflammation induced by suboptimal vaccination (Fig. 6E to G and I). This suggests a more complex regulatory mechanism for those mediators by cell types other than $CD4^+$ T cells, depending on the antigen concentration. Interestingly, we did not find a role for TNF-α in low-antigen-dose-mediated ERD. TNF-α has been identified as a key cytokine mediating weight loss and airway obstruction in FI-RSV-induced ERD in mice (19). In contrast, $CD4^+$ T cell depletion in mice immunized with low RSV F doses did not impact TNF-α levels (Fig. 6D) but profoundly impacted the observed histopathology (Fig. 9).

It could be hypothesized that both the Th17 and Th2 $CD4^+$ T cell subsets are responsible for FI-RSV-induced ERD and that the Th17 $CD4^+$ T cell subset is mainly responsible for ERD induced by low RSV F vaccine doses, but additional investigations are needed to further characterize the $CD4^+$ T cell subset responsible for low-antigen-dose-induced ERD.

In summary, we have confirmed in the mouse model the safety signals associated with low-dose immunization with RSV post-F plus GLA-SE. Our initial observations, therefore, were likely not specific to the cotton rat model alone. Further investigations are still needed to fully uncover the mechanism associated with low-antigen-dose-induced ERD. Importantly, these results might relate to heterogeneous responses to vaccination that are likely

FIG 7 Legend (Continued)
GLA-SE (2.5 μg GLA in 2% SE) as an adjuvant, or FI-RSV. A negative-control group was immunized with a nonrelevant antigen (CMV gB) with GLA-SE as an adjuvant. Naïve animals were left untreated. At days 29, 32, and 35, groups shown in orange were treated i.p. with 250 μg of anti-CD8 antibodies. Four days after i.n. challenge with 10^6 PFU of wild-type (wt) RSV A2, animals were sacrificed. Lungs were homogenized and clarified, and individual supernatants were analyzed by multiplex assays to assess the respective concentrations of eotaxin (A), IL-5 (B), IL-13 (C), TNF-α (D), IL-6 (E), IP-10 (F), MCP-1 (G), IL-17 (H), KC (I), and MIP-2 (J). Individual values and median with ranges are shown. Kruskal-Wallis analysis followed by Dunn's multiple-comparison tests was used for statistical analyses. Symbols indicate an adjusted *P* value of <0.05 for nondepleted conditions compared to buffer alone (#) or a *P* value of <0.05 for pairwise Mann-Whitney tests comparing nondepleted with CD8 T cell-depleted conditions (*).

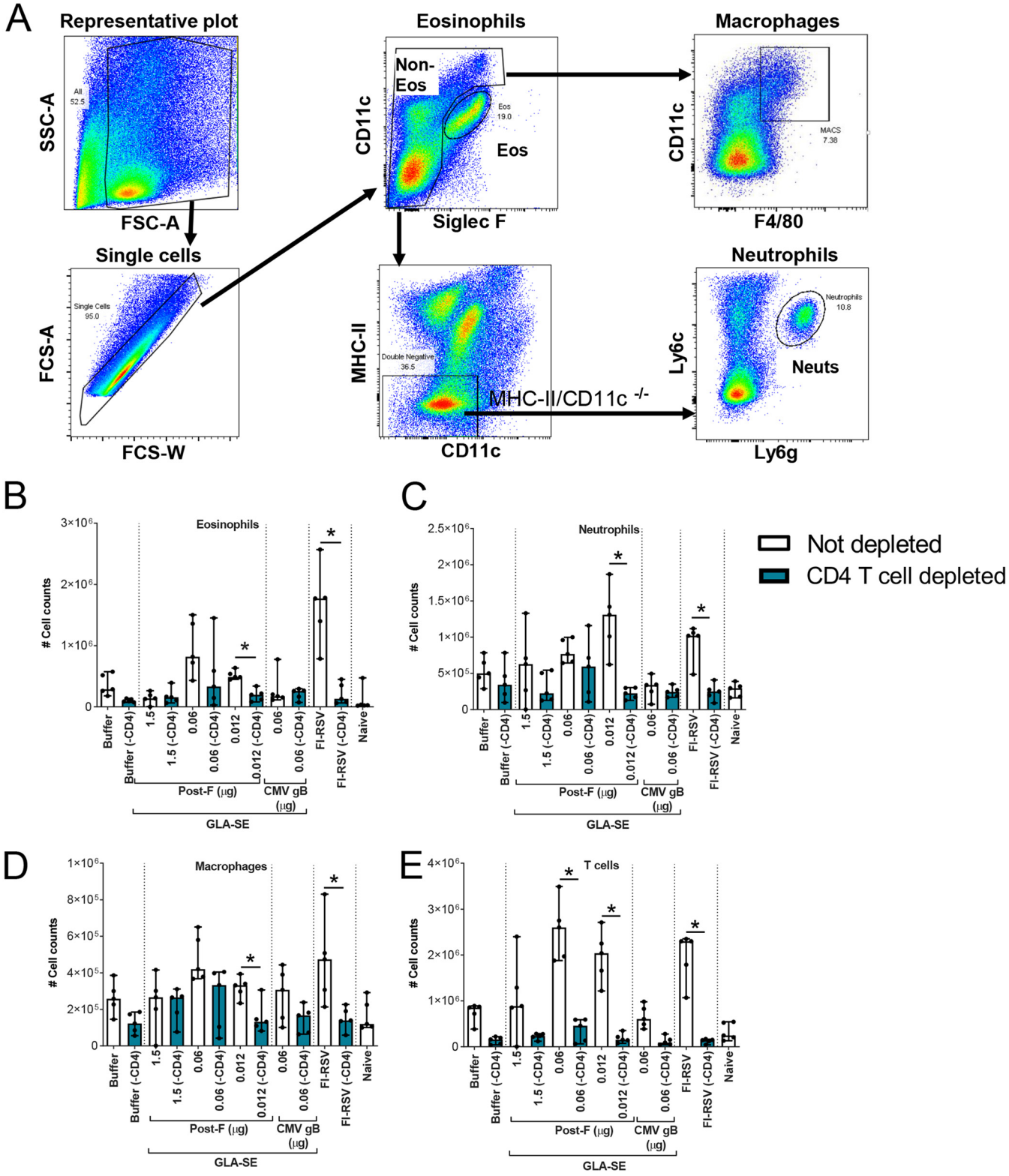

FIG 8 CD4+ T cell depletion strongly reduces inflammatory cell infiltration into the lungs postchallenge. BALB/c mice (7 weeks old; *n*, 5 per group) were immunized i.m. at day 0 and day 21 with either buffer alone, different doses of post-F antigen with GLA-SE (2.5 μg GLA in 2% SE) as an adjuvant, or FI-RSV. A negative-control group was immunized with a nonrelevant antigen (CMV gB) with GLA-SE as an adjuvant. Naïve animals were left untreated. At days 29, 32, and 35, animals were treated i.p. with 250 μg of anti-CD4 antibodies. At day 34, animals were challenged i.n. with 10^6 PFU of wild-type (wt) RSV A2, and 4 days later, animals were sacrificed. Lungs were harvested, and cells were isolated and surface stained as described in Materials and Methods. (A) Gating strategy for the assessment of cells infiltrating the lungs. SSC, side scatter; FSC, forward scatter. (B through E) Total numbers of eosinophils (B), neutrophils (C), macrophages (D), and T cells (E), calculated on the basis of flow cytometry results and total cell counts. For statistical analyses, pairwise Mann-Whitney tests comparing nondepleted with CD4 T cell-depleted conditions were performed. *, $P < 0.05$. Individual results and medians with ranges are shown.

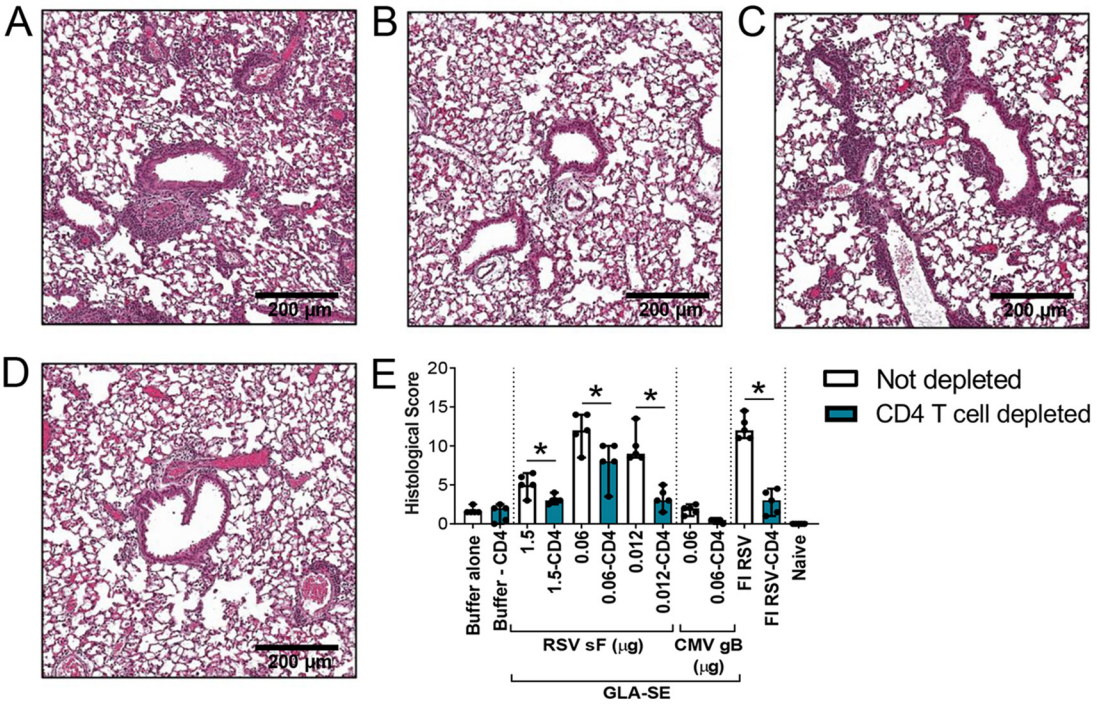

FIG 9 Histological examination confirms that CD4$^+$ T cell depletion inhibits the enhanced lung pathology induced by vaccination with low antigen doses or FI-RSV. BALB/c mice (7 weeks old; *n*, 5 per group) were immunized i.m. at day 0 and day 21 with either buffer alone, different doses of post-F antigen with GLA-SE (2.5 μg GLA in 2% SE) as an adjuvant, or FI-RSV. A negative-control group was immunized with a nonrelevant antigen (CMV gB) with GLA-SE as an adjuvant. Naïve animals were left untreated. At days 29, 32, and 35, animals were treated i.p. with 250 μg of anti-CD4 antibodies. At day 34, animals were challenged i.n. with 10^6 PFU of wild-type (wt) RSV A2, and 4 days later, animals were sacrificed. Lungs were harvested, inflated with 10% formalin, and embedded in paraffin. (A through D) Photomicrographs of H&E-stained sections are shown at $\times$10 magnification for animals vaccinated with 0.012 μg RSV sF (A), 0.012 μg RSV sF plus anti-CD4 (B), FI-RSV (C), or FI-RSV plus anti-CD4 (D). (E) Lung histopathology was analyzed blindly by a trained pathologist; the combined scores are presented for all groups as medians with ranges of individual results. Pairwise Mann-Whitney analyses comparing nondepleted with CD4 T cell-depleted conditions were performed on histopathology scores. *, $P < 0.05$.

to be observed in humans, in the case of a poor response to vaccine or in the context of a waning of the immune response. While it is not clear whether suboptimally dosed rodents are an appropriate model for such responses, our findings indicate the need for great care in any study of subunit RSV vaccines in naïve children.

MATERIALS AND METHODS

Ethics statement. All procedures were performed in accordance with federal, state, and institutional guidelines in an AAALAC-accredited facility, The MedImmune Institutional Animal Care and Use Committee (IACUC) board approved this research under a specified protocol (MI-16-0004), and all animal work was performed in accordance with the IACUC policies. MedImmune is registered with the U.S. Department of Agriculture (USDA) and applies the standards outlined in the *Guide for the Care and Use of Laboratory Animals* (29) to its institutional animal care and use program. Animals were lightly anesthetized with isoflurane for immunizations and blood draws and were euthanized with carbon dioxide for terminal organ harvests.

Vaccine components. The soluble RSV post-F and cytomegalovirus gB antigens were produced as described previously (16, 30). GLA-SE (31) was licensed from Immune Design Corporation (Seattle, WA) and was used at 2.5 μg GLA in 2% SE per dose. FI-RSV was obtained from Sigmovir Biosystems (Rockville, MD) and was prepared as described previously (16). RSV A2 (ATCC) was propagated on HEp-2 cells (ATCC) grown in Eagle's minimum essential medium (EMEM). Supernatants were spun to remove cell debris, and the virus was stabilized with 1$\times$ sucrose phosphate (0.2 M sucrose, 0.0038 M KH_2PO_4, and 0.0072 M K_2HPO_4) before snap-freezing in 1.5-ml aliquots and storage at -80°C until use.

Animals, immunizations, CD4$^+$ T cell depletions, and RSV challenge. Seven-week-old female BALB/c mice (Envigo, Dublin, VA) were housed under pathogen-free conditions at MedImmune (Gaithersburg, MD). Immunizations with RSV F, FI-RSV, and the negative controls cytomegalovirus (CMV) glycoprotein B (gB) and protein storage buffer (20 mM histidine and histidine HCl, 23 mM potassium chloride, 7% [wt/vol] sucrose, 0.01% polysorbate 80 [pH 6.5]) were administered by i.m. injection on days 0 and 21. Animals were challenged intranasally under isoflurane anesthesia with RSV A2 (1×10^6 PFU) on day 34 and were terminated on day 38. The naïve group remained untreated. To deplete CD4$^+$ or CD8$^+$

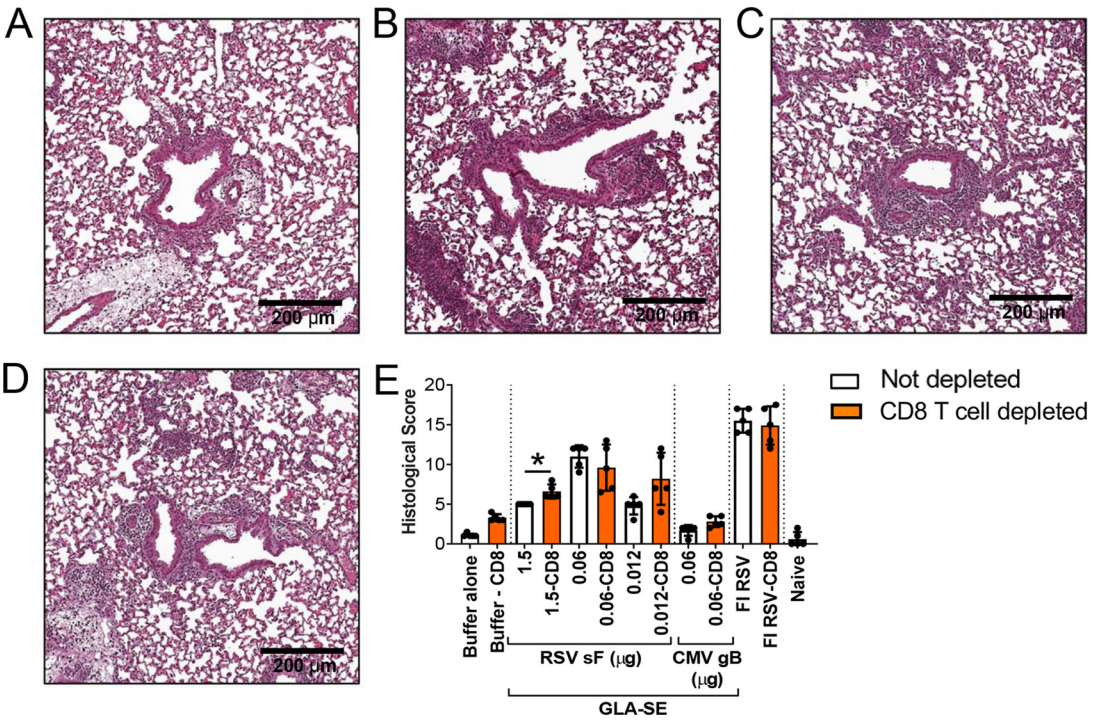

FIG 10 Histological examination confirms that CD8+ T cell depletion does not inhibit the enhanced lung pathology induced by vaccination with low antigen doses or FI-RSV. BALB/c mice (7 weeks old; *n*, 5 per group) were immunized i.m. at day 0 and day 21 with either buffer alone, different doses of post-F antigen with GLA-SE (2.5 μg GLA in 2% SE) as an adjuvant, or FI-RSV. A negative-control group was immunized with a nonrelevant antigen (CMV gB) with GLA-SE as an adjuvant. Naïve animals were left untreated. At days 29, 32, and 35, some groups were treated i.p. with 250 μg of anti-CD8 antibodies. At day 34, animals were challenged i.n. with 10^6 PFU of wild-type (wt) RSV A2, and 4 days later, animals were sacrificed. Lungs were harvested, inflated with 10% formalin, and embedded in paraffin. (A to D) Photomicrographs of H&E-stained sections are shown at ×10 magnification for animals vaccinated with 0.012 μg RSV sF (A), 0.012 μg RSV sF plus anti-CD8 (B), FI-RSV (C), or FI-RSV plus anti-CD8 (D). (E) Lung histopathology was analyzed blindly by a trained pathologist; the combined scores are presented for all groups as medians with ranges of individual results. Pairwise Mann-Whitney analyses of nondepleted versus CD8 T cell-depleted conditions were performed on histology scores. *, $P < 0.05$.

T cells, mice received three injections of anti-mouse CD4 antibodies (clones GK1.5 and YTS191) from Bio X Cell (West Lebanon, NH) at 250 μg each or an anti-mouse CD8+ antibody at 250 μg (clone 53-5.8) from BioLegend (San Diego, CA) on days 29, 32, and 35 by intraperitoneal (i.p.) injection. The efficiency of CD4+ and CD8+ depletion in the lungs was confirmed by flow cytometry after termination. Different antibody clones were used for flow cytometry and depletion.

Microneutralization assay. Serum samples were heat inactivated at 56°C for 45 min. In 96-well plates, the positive-control antibody (palivizumab) was serially diluted by 3-fold increments (starting at 8 μg/ml) in cell culture medium (minimal essential medium [MEM] supplemented with 5% heat-inactivated fetal bovine serum [FBS], 2 mM L-glutamine, 100 U of penicillin/ml, and 100 μg of streptomycin/ml [all from Invitrogen]) for a final volume of 50 μl. In duplicate, the test sera (starting dilution, 1:8) were serially diluted by 3-fold increments in cell culture medium for a final volume of 50 μl. A 25-μl volume of cell culture medium was added to the first dilution to bring the volume back to 50 μl, bringing the starting dilution down to 1:16. Each serum dilution was mixed with 50 μl RSV A2 at 500 PFU per well. Following 2 h of incubation at 37°C under 5% CO_2, 2.5×10^4 HEp-2 cells in a 100-μl volume were added to each well. Cell-plus-virus and cell-only wells served as controls. After 3 days of incubation at 37°C under 5% CO_2, the cell culture medium was removed, and the monolayer was fixed with chilled 80% acetone. RSV replication was visualized by immunostaining with a horseradish peroxidase (HRP)-labeled monoclonal antibody, 1331H (32). The reciprocal $\log_2$ of the 50% inhibitory concentration (IC_{50}) was determined for each serum sample using GraphPad Prism software (version 7.02). The lower limit of detection (LLOD) of this assay is 4 $\log_2$. If an IC_{50} value could not be calculated, the $\log_2$ of the initial dilution (1:16) was used for analysis.

Serum IgG ELISA. Serological responses were evaluated by a standard enzyme-linked immunosorbent assay (ELISA) with sera collected at the day of sacrifice on plates coated with RSV post-F (100 ng/well) plates. Control antibodies (purified 1331H for total IgG) (32) were serially diluted by 3-fold increments starting from a concentration of 1 μg/ml in sample diluent (phosphate-buffered saline [PBS] with 1% bovine serum albumin [BSA] and 0.05% Tween 20). Samples were diluted in sample diluent at $1:10^2$ to $1:10^7$. Bound total IgG was detected with an HRP-labeled goat anti-mouse IgG antibody (Dako). The serum antibody concentrations were calculated (in micrograms per milliliter) based on the standard curves (SoftMax Pro, version 5.4).

Lung and NT processing for plaque assays, cytokine assessment, and histology. Lungs or nasal turbinates (NT) were collected 4 days post-RSV challenge. For the plaque assay, the inferior right lung lobe was tied off and cut below the tie. Lung lobes and NT were placed in cold Hanks balanced salt solution supplemented with 1× sucrose phosphate in tissue homogenization tubes (MP Biomedicals) and were homogenized using an MP FastPrep-24 instrument (MP Biomedicals). The clarified supernatants were serially diluted and placed onto subconfluent HEp-2 cells in 24-well plates. After 90 min of incubation, supernatants were removed. and cells were overlaid with MEM–FBS–penicillin-streptomycin supplemented with 0.75% methylcellulose. After 5 days, cells were fixed with 100% methanol for 15 min. Following fixation, cells were blocked for 1 h in 5% nonfat milk and were stained for 1 h with a goat polyclonal antibody against RSV (Chemicon), followed by staining for 1 h with an HRP-conjugated rabbit anti-goat antibody (Dako). To visualize plaques, cells were incubated with a ready-to-use 3-amino-9-ethylcarbazole (AEC) substrate system (Dako), followed by a water rinsing step. PFU per gram were calculated based on the number of plaques, dilution factors, and tissue weight. For cytokine assessment, multiplex analysis of cytokine expression levels was conducted on 25 μl of lung homogenate supernatant according to the manufacturer's instructions (Bio-Rad, Hercules, CA). Values below the LLOD were analyzed as zero. For histology, the remaining four lobes of the lung were inflated using a tracheal cannula, fixed with 10% neutral formalin, and processed in paraffin. Tissues were sectioned at 4 μm, mounted on polarized slides, and stained with hematoxylin and eosin (H&E) for histologic evaluation on a Nikon Eclipse 80i light microscope by a board-certified pathologist.

Flow cytometry. Lung cells were collected 4 days postchallenge and were isolated as described previously (33), except that lungs were processed with a gentleMACS dissociator (Miltenyi Biotec) in 5 ml digestion buffer rather than being manually dissociated and were incubated at 37°C for 30 min.

Eosinophils were stained and gated as described previously (21). Cells were surface stained with antibodies specific to Ly6c (clone HK1.4; BioLegend), Siglec F (clone E50-2440; BD Biosciences), Ly6g (clone 1A8; BioLegend), major histocompatibility complex class II (MHC-II) (clone M5/114.15.2; BioLegend), CD11c (clone N418; BioLegend), CD11b (clone M1/70; eBioscience), F4/80 (clone BM8; eBioscience), and CD45 (clone 30-F11; BioLegend) for 30 min at 4°C and were fixed with fixation buffer (eBioscience). A total of 300,000 events were collected on a BD FACS LSR II instrument and were analyzed using FlowJo software (Tree Star, Ashland, OR).

For intracellular cytokine staining (ICS), cells were incubated with 1 μg/ml of overlapping RSV F peptide pools (JPT, Berlin, Germany) for 12 h in the presence of 10 μg/ml brefeldin A (BFA) (BD Biosciences) at 37°C. Following stimulation, cells were blocked with CD16/32 (BD Biosciences) and were stained with a fixable Live/Dead dye (Thermo Fisher) for 20 min. Cells were then surface stained with antibodies specific to CD4 (clone RM4-5; BD Biosciences), CD8 (clone 53-6.7; BD Biosciences), and CD 19 (clone 6D5; BioLegend) for 20 min. The antibody clones used for fluorescence-activated cell sorter (FACS) staining recognized epitopes different from those for the antibody clones used for depletion. Cells were fixed and permeabilized with a BD Biosciences kit (catalog no. 554715) and were stained intracellularly for CD3 (BioLegend), IFN-γ (clone XMG1.2; BD Biosciences), TNF-α (clone MP6-XT22; BD Biosciences), and IL-2 (clone JES6-5H4; BD Biosciences). A total of 500,000 events were collected on a BD FACS LSR II instrument and were analyzed using FlowJo software (Tree Star, Ashland, OR). The total number of cytokine-producing cells was calculated after subtraction of background staining using BFA-only controls. Total cell counts were calculated from total cell counts in the lungs, performed on a Guava EasyCyte Plus flow cytometer with ViaCount beads.

Statistical analysis. Sample size estimation was assessed with 80% power to detect differences between treatment groups (based on pilot data) using a two-group Satterthwaite *t* test with a two-sided significance level of 0.05, prior to experimentation. Sample sizes were estimated using nQuery Advisor+ nTerim 3.0. When all group values were approximately equal to the LLOD, no statistical analysis was performed. When two groups were compared, Mann-Whitney tests were performed. When three or more groups were compared, Kruskal-Wallis tests were performed, followed by Dunn's posttests where multiplicity-adjusted two-sided *P* values are reported. A *P* value of <0.05 was considered significant. Analyses were performed with GraphPad Prism, version 8.1.0.

ACKNOWLEDGMENTS

We acknowledge JoAnn Suzich for critical reviews of the manuscript. We also thank Sally Lee and Holly Koelkebeck (MedImmune Histology Laboratory) for processing and staining all the mouse lungs from all our ERD studies.

We have no conflict of interest to declare.

The work was funded by MedImmune, LLC, but the funders had no role in study design, data collection and analysis, decision to publish, or preparation of the manuscript.

REFERENCES

1. Ebbert JO, Limper AH. 2005. Respiratory syncytial virus pneumonitis in immunocompromised adults: clinical features and outcome. Respiration 72:263–269. https://doi.org/10.1159/000085367.
2. Hall CB, Weinberg GA, Iwane MK, Blumkin AK, Edwards KM, Staat MA, Auinger P, Griffin MR, Poehling KA, Erdman D, Grijalva CG, Zhu Y, Szilagyi P. 2009. The burden of respiratory syncytial virus infection in young children. N Engl J Med 360:588–598. https://doi.org/10.1056/NEJMoa0804877.
3. Widmer K, Zhu Y, Williams JV, Griffin MR, Edwards KM, Talbot HK. 2012.

Rates of hospitalizations for respiratory syncytial virus, human metapneumovirus, and influenza virus in older adults. J Infect Dis 206:56–62. https://doi.org/10.1093/infdis/jis309.
4. The IMpact-RSV Study Group. 1998. Palivizumab, a humanized respiratory syncytial virus monoclonal antibody, reduces hospitalization from respiratory syncytial virus infection in high-risk infants. Pediatrics 102:531–537. https://doi.org/10.1542/peds.102.3.531.
5. Chin J, Magoffin RL, Shearer LA, Schieble JH, Lennette EH. 1969. Field evaluation of a respiratory syncytial virus vaccine and a trivalent parainfluenza virus vaccine in a pediatric population. Am J Epidemiol 89:449–463. https://doi.org/10.1093/oxfordjournals.aje.a120957.
6. Fulginiti VA, Eller JJ, Sieber OF, Joyner JW, Minamitani M, Meiklejohn G. 1969. Respiratory virus immunization. I. A field trial of two inactivated respiratory virus vaccines; an aqueous trivalent parainfluenza virus vaccine and an alum-precipitated respiratory syncytial virus vaccine. Am J Epidemiol 89:435–448. https://doi.org/10.1093/oxfordjournals.aje.a120956.
7. Kapikian AZ, Mitchell RH, Chanock RM, Shvedoff RA, Stewart CE. 1969. An epidemiologic study of altered clinical reactivity to respiratory syncytial (RS) virus infection in children previously vaccinated with an inactivated RS virus vaccine. Am J Epidemiol 89:405–421. https://doi.org/10.1093/oxfordjournals.aje.a120954.
8. Kim HW, Canchola JG, Brandt CD, Pyles G, Chanock RM, Jensen K, Parrott RH. 1969. Respiratory syncytial virus disease in infants despite prior administration of antigenic inactivated vaccine. Am J Epidemiol 89:422–434. https://doi.org/10.1093/oxfordjournals.aje.a120955.
9. Murphy BR, Walsh EE. 1988. Formalin-inactivated respiratory syncytial virus vaccine induces antibodies to the fusion glycoprotein that are deficient in fusion-inhibiting activity. J Clin Microbiol 26:1595–1597.
10. Acosta PL, Caballero MT, Polack FP. 2015. Brief history and characterization of enhanced respiratory syncytial virus disease. Clin Vaccine Immunol 23:189–195. https://doi.org/10.1128/CVI.00609-15.
11. Hurwitz JL. 2011. Respiratory syncytial virus vaccine development. Expert Rev Vaccines 10:1415–1433. https://doi.org/10.1586/erv.11.120.
12. McLellan JS, Chen M, Joyce MG, Sastry M, Stewart-Jones GB, Yang Y, Zhang B, Chen L, Srivatsan S, Zheng A, Zhou T, Graepel KW, Kumar A, Moin S, Boyington JC, Chuang GY, Soto C, Baxa U, Bakker AQ, Spits H, Beaumont T, Zheng Z, Xia N, Ko SY, Todd JP, Rao S, Graham BS, Kwong PD. 2013. Structure-based design of a fusion glycoprotein vaccine for respiratory syncytial virus. Science 342:592–598. https://doi.org/10.1126/science.1243283.
13. Anderson LJ, Dormitzer PR, Nokes DJ, Rappuoli R, Roca A, Graham BS. 2013. Strategic priorities for respiratory syncytial virus (RSV) vaccine development. Vaccine 31(Suppl 2):B209–B215. https://doi.org/10.1016/j.vaccine.2012.11.106.
14. Christiaansen AF, Knudson CJ, Weiss KA, Varga SM. 2014. The CD4 T cell response to respiratory syncytial virus infection. Immunol Res 59:109–117. https://doi.org/10.1007/s12026-014-8540-1.
15. Shaw CA, Ciarlet M, Cooper BW, Dionigi L, Keith P, O'Brien KB, Rafie-Kolpin M, Dormitzer PR. 2013. The path to an RSV vaccine. Curr Opin Virol 3:332–342. https://doi.org/10.1016/j.coviro.2013.05.003.
16. Schneider-Ohrum K, Cayatte C, Bennett AS, Rajani GM, McTamney P, Nacel K, Hostetler L, Cheng L, Ren K, O'Day T, Prince GA, McCarthy MP. 2017. Immunization with low doses of recombinant postfusion or prefusion respiratory syncytial virus F primes for vaccine-enhanced disease in the cotton rat model independently of the presence of a Th1-biasing (GLA-SE) or Th2-biasing (alum) adjuvant. J Virol 91:e02180-16. https://doi.org/10.1128/JVI.02180-16.
17. Waris ME, Tsou C, Erdman DD, Zaki SR, Anderson LJ. 1996. Respiratory syncytial virus infection in BALB/c mice previously immunized with formalin-inactivated virus induces enhanced pulmonary inflammatory response with a predominant Th2-like cytokine pattern. J Virol 70:2852–2860.
18. Power UF, Huss T, Michaud V, Plotnicky-Gilquin H, Bonnefoy JY, Nguyen TN. 2001. Differential histopathology and chemokine gene expression in lung tissues following respiratory syncytial virus (RSV) challenge of formalin-inactivated RSV- or BBG2Na-immunized mice. J Virol 75:12421–12430. https://doi.org/10.1128/JVI.75.24.12421-12430.2001.
19. Knudson CJ, Hartwig SM, Meyerholz DK, Varga SM. 2015. RSV vaccine-enhanced disease is orchestrated by the combined actions of distinct CD4 T cell subsets. PLoS Pathog 11:e1004757. https://doi.org/10.1371/journal.ppat.1004757.
20. Laan M, Cui ZH, Hoshino H, Lotvall J, Sjostrand M, Gruenert DC, Skoogh BE, Linden A. 1999. Neutrophil recruitment by human IL-17 via C-X-C chemokine release in the airways. J Immunol 162:2347–2352.
21. Castilow EM, Legge KL, Varga SM. 2008. Eosinophils do not contribute to respiratory syncytial virus vaccine-enhanced disease. J Immunol 181:6692–6696. https://doi.org/10.4049/jimmunol.181.10.6692.
22. Stevens WW, Kim TS, Pujanauski LM, Hao X, Braciale TJ. 2007. Detection and quantitation of eosinophils in the murine respiratory tract by flow cytometry. J Immunol Methods 327:63–74. https://doi.org/10.1016/j.jim.2007.07.011.
23. Boukhvalova MS, Blanco JC. 2013. The cotton rat Sigmodon hispidus model of respiratory syncytial virus infection. Curr Top Microbiol Immunol 372:347–358. https://doi.org/10.1007/978-3-642-38919-1_17.
24. Rey GU, Miao C, Caidi H, Trivedi SU, Harcourt JL, Tripp RA, Anderson LJ, Haynes LM. 2013. Decrease in formalin-inactivated respiratory syncytial virus (FI-RSV) enhanced disease with RSV G glycoprotein peptide immunization in BALB/c mice. PLoS One 8:e83075. https://doi.org/10.1371/journal.pone.0083075.
25. Olson MR, Varga SM. 2007. CD8 T cells inhibit respiratory syncytial virus (RSV) vaccine-enhanced disease. J Immunol 179:5415–5424. https://doi.org/10.4049/jimmunol.179.8.5415.
26. Graham BS, Davis TH, Tang YW, Gruber WC. 1993. Immunoprophylaxis and immunotherapy of respiratory syncytial virus-infected mice with respiratory syncytial virus-specific immune serum. Pediatr Res 34:167–172. https://doi.org/10.1203/00006450-199308000-00013.
27. Connors M, Kulkarni AB, Firestone CY, Holmes KL, Morse HC, III, Sotnikov AV, Murphy BR. 1992. Pulmonary histopathology induced by respiratory syncytial virus (RSV) challenge of formalin-inactivated RSV-immunized BALB/c mice is abrogated by depletion of CD4+ T cells. J Virol 66:7444–7451.
28. Zhang L, Li H, Hai Y, Yin W, Li W, Zheng B, Du X, Li N, Zhang Z, Deng Y, Zeng R, Wei L. 2017. CpG in combination with an inhibitor of Notch signaling suppresses formalin-inactivated respiratory syncytial virus-enhanced airway hyperresponsiveness and inflammation by inhibiting Th17 memory responses and promoting tissue-resident memory cells in lungs. J Virol 91:e02111-16. https://doi.org/10.1128/JVI.02111-16.
29. National Research Council. 2011. Guide for the care and use of laboratory animals, 8th ed. National Academies Press, Washington, DC.
30. Cayatte C, Schneider-Ohrum K, Wang Z, Irrinki A, Nguyen N, Lu J, Nelson C, Servat E, Gemmell L, Citkowicz A, Liu Y, Hayes G, Woo J, Van Nest G, Jin H, Duke G, McCormick AL. 2013. Cytomegalovirus vaccine strain Towne-derived dense bodies induce broad cellular immune responses and neutralizing antibodies that prevent infection of fibroblasts and epithelial cells. J Virol 87:11107–11120. https://doi.org/10.1128/JVI.01554-13.
31. Anderson RC, Fox CB, Dutill TS, Shaverdian N, Evers TL, Poshusta GR, Chesko J, Coler RN, Friede M, Reed SG, Vedvick TS. 2010. Physicochemical characterization and biological activity of synthetic TLR4 agonist formulations. Colloids Surf B Biointerfaces 75:123–132. https://doi.org/10.1016/j.colsurfb.2009.08.022.
32. Beeler JA, van Wyke Coelingh K. 1989. Neutralization epitopes of the F glycoprotein of respiratory syncytial virus: effect of mutation upon fusion function. J Virol 63:2941–2950.
33. Schneider-Ohrum K, Giles BM, Weirback HK, Williams BL, DeAlmeida DR, Ross TM. 2011. Adjuvants that stimulate TLR3 or NLPR3 pathways enhance the efficiency of influenza virus-like particle vaccines in aged mice. Vaccine 29:9081–9092. https://doi.org/10.1016/j.vaccine.2011.09.051.